

# Cyanidin 3-Glucoside Induces Hepatocyte Growth Factor in Normal Human Dermal Fibroblasts through the Activation of $\beta_2$ -Adrenergic Receptor

Annisa Krama, Natsu Tokura, Hiroko Isoda, Hideyuki Shigemori, and Yusaku Miyamae\*



Cite This: *ACS Omega* 2022, 7, 22889–22895



Read Online

ACCESS |



Metrics & More

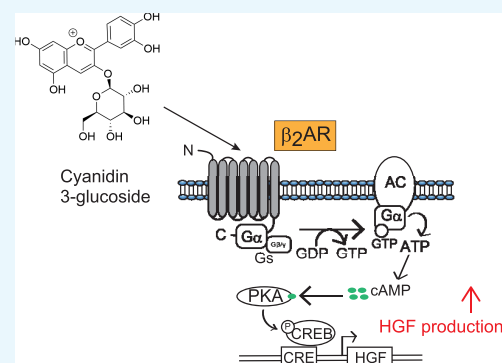


Article Recommendations



Supporting Information

**ABSTRACT:** Hepatocyte growth factor (HGF) is expressed in various organs and involved in the fundamental cellular functions such as mitogenic, motogenic, and morphogenic activities. Induction of HGF may be therapeutically useful for controlling organ regeneration, wound healing, and embryogenesis. In this study, we examined the stimulation effect of cyanidin 3-glucoside (C3G), an anthocyanidin derivative, on HGF production in normal human dermal fibroblasts (NHDFs) and the underlying mechanisms. C3G induced HGF production at both mRNA and protein levels in NHDF cells and enhanced the phosphorylation of cAMP-response element-binding protein. We also observed that treatment with C3G increased intracellular cAMP level and promoter activity of cAMP-response element in HEK293 cells expressing  $\beta_2$ -adrenergic receptor ( $\beta_2$ AR). In contrast, cyanidin, an aglycon of C3G, did not show the activation of  $\beta_2$ AR signaling and HGF production. These results indicate that C3G behaves as an agonist for  $\beta_2$ AR signaling to activate the protein kinase A pathway and induce the production of HGF.



## INTRODUCTION

Hepatocyte growth factor (HGF) was first discovered as a mitogenic protein from rat hepatocytes, which showed regenerative effects in the injured liver.<sup>1</sup> HGF is produced as a single chain pro-HGF, which is cleaved into active HGF.<sup>2</sup> In the normal state, active HGF binds to its receptor, *c*-Met, and stimulates various biological responses such as proliferation, cell survival, morphogenesis, motility, and angiogenesis.<sup>3,4</sup> Therefore, HGF is recognized as a potential therapeutic agent for various diseases, especially hepatic and renal fibrosis and cardiovascular diseases.<sup>5</sup> Moreover, migration and proliferation of keratinocytes can be stimulated by HGF, suggesting the involvement in cutaneous physiology and wound healing.<sup>6,7</sup> Some reports also highlighted the therapeutic potential of HGF in neuronal diseases such as amyotrophic lateral sclerosis and Alzheimer's disease by demonstrating that exogenous expression of HGF-regulated neuronal cell survival.<sup>8,9</sup> These studies motivate us to search the small molecules that function as HGF inducers for potential therapeutic tools.

Production of HGF is regulated by several signaling pathways, including protein kinase A (PKA), protein kinase C (PKC), and mitogen-activated protein kinases (MAPKs).<sup>10,11</sup> Gohda and his colleagues reported that the extract of bitter melon pulp (*Momordica charantia* L.) stimulated the HGF production in normal human dermal fibroblasts (NHDFs).<sup>12</sup> They demonstrated that the extract upregulated *HGF* gene expression through the activation of extracellular signal-regulated kinase (ERK), whereas the active

components have not been identified yet. We also found that naturally occurring compounds, such as caffeoylquinic acids (CQAs), acteoside, and daphnane diterpenoids, acted as HGF inducers in NHDFs.<sup>13,14</sup> However, the mechanisms underlying HGF production and target molecules of these pure natural compounds have not been identified yet.

During our search for new HGF inducers from natural products, we found that cyanidin 3-glucoside (C3G; Figure 1A) promoted the production of HGF in NHDFs. C3G is the most common anthocyanidins found in edible fruits, legumes, grains, and many colorful vegetables<sup>15</sup> and has been known to possess various biological activities such as antioxidant, anti-inflammation, antidiabetic, and antiobesity effects.<sup>16–18</sup> However, the effects of C3G on HGF production and potential binding protein have not been clarified. Here, we report that C3G enhances the HGF production in NHDFs through the elevation of cAMP level and activation of PKA pathway possibly by targeting  $\beta_2$ -adrenergic receptor ( $\beta_2$ AR).

Received: April 29, 2022

Accepted: June 7, 2022

Published: June 22, 2022



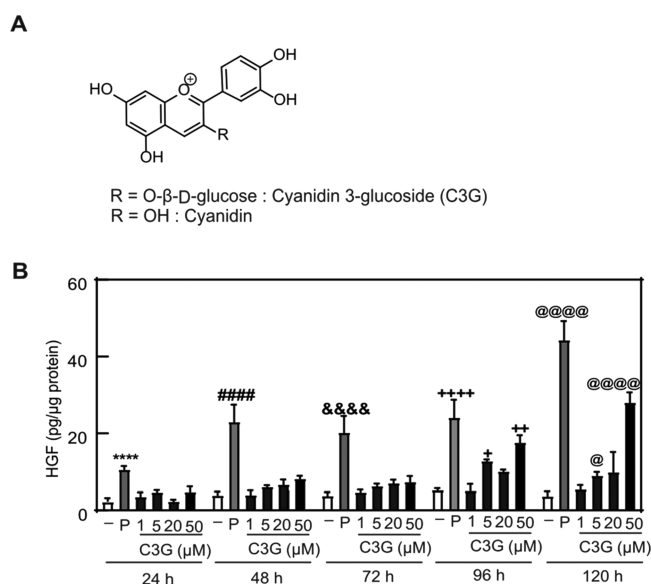


**Figure 1.** Effect of C3G on HGF production in NHDF cells. (A) Chemical structures of C3G and cyanidin. (B) NHDF cells were treated with vehicle (0.1% DMSO, shown as -), PDGF-BB (25 ng/mL, shown as P), or C3G at the indicated concentrations and monitored over time. The amount of HGF secreted into the culture medium was determined by an ELISA assay. Statistical analysis was conducted using one-way ANOVA analysis (Tukey's test). Significant differences ( $p < 0.0001$ ) versus vehicle at 24 h (\*\*\*\*), 48 h (#####), 72 h (&&&&), 96 h (++++), 120 h (@@@@). Significant difference ( $p < 0.01$ ) versus vehicle at 96 h (++) and 120 h (@).  $n = 5$ .

## RESULTS

**Effect of C3G on HGF Production in NHDF Cells.** To examine the effects of C3G on HGF production levels in NHDFs, we initially tested the viability of C3G-treated cells by using an MTT assay. C3G did not show the cytotoxicity against NHDFs at concentrations of 0.1–50  $\mu$ M in treatments for 24, 48, and 120 h (Figure S1). Next, we performed an ELISA assay to quantify the levels of HGF secreted to the culture medium of the NHDFs treated with different concentrations (1, 5, 20, and 50  $\mu$ M) of C3G in various incubation time (24, 48, 72, 96, and 120 h). Platelet-derived growth factor-BB (PDGF-BB) (25 ng/mL) was used as a positive control to stimulate intracellular HGF levels.<sup>19</sup> In our results, C3G stimulated the HGF production in a dose-dependent manner at each treatment time (Figure 1B). The maximum dose (50  $\mu$ M) of C3G also showed a time-dependent increase of HGF levels. These results clearly showed the promoting effect of C3G on HGF production.

To obtain more evidence for the stimulation of HGF production by C3G, the expression level of *HGF* genes was investigated by a real-time RT-PCR. The treatment of C3G at 50  $\mu$ M increased mRNA abundance of *HGF* genes almost twice as much as vehicle control (Figure 2), suggesting that C3G upregulated the transcription of *HGF* genes.

**Effects of C3G on PKA Pathway and Phosphorylation of CREB.** To identify the signaling pathway involved in C3G-mediated HGF induction, we tested whether the effect of C3G on HGF production was canceled by co-treatment of selective signaling transduction inhibitor. We found that the induction of HGF by C3G was suppressed in the presence of H89 (Figure 3A), a PKA pathway inhibitor that blocks the binding

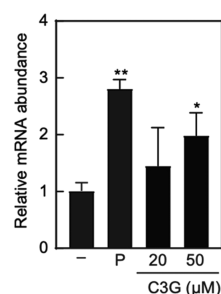


**Figure 2.** Effect of C3G on mRNA expression of HGF gene. NHDF cells were treated with vehicle (0.1% DMSO, shown as -), PDGF-BB (shown as P), or C3G at the indicated concentrations for 48 h. Relative mRNA abundance was measured by using a real-time RT-PCR. The mRNA levels of *HGF* were calculated as relative levels compared with  $\beta$ -actin. Statistical analysis was conducted using Student's t-test analysis. Significant difference (\*\* $p < 0.01$ , \* $p < 0.05$ ) versus vehicle.  $n = 3$ .

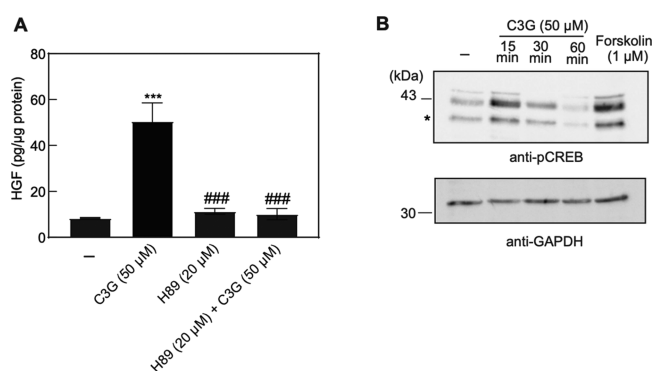


**Figure 3.** Effect of C3G on the PKA pathway. (A) NHDF cells were treated with vehicle (0.1% DMSO, shown as -), C3G, and H89 at the indicated concentrations for 120 h. The amount of HGF secreted into the culture medium was measured by ELISA assay. Statistical analysis was conducted using one-way ANOVA analysis (Tukey's test). Significant differences ( $p < 0.01$ ) versus vehicle (\*\*\*) or C3G treatment group (###).  $n = 5$ . (B) NHDF cells were treated with C3G (50  $\mu$ M) for 15, 30, or 60 min, and forskolin (1  $\mu$ M) for 15 min. DMSO (0.1%) was used for vehicle group treatment (shown as -). Cell lysates were immunoblotted with antibody against p-CREB. GAPDH is used for loading control. The asterisk (\*) indicates the phosphorylated form of ATF-1 at Ser63.

of ATP on PKA catalytic subunit.<sup>20</sup> In contrast, the promoting effect of HGF by C3G was not canceled by co-treatment of other inhibitors, which target the PKC and MAPK pathways (data not shown). These suggested that C3G selectively activated the PKA pathway for the induction of HGF levels. To further confirm the effect of C3G on the PKA pathway, we examined the phosphorylation of cAMP-response element-binding protein (CREB) by using western blotting analysis. Ser133 residue of the CREB is phosphorylated by the activated PKA kinase followed by the elevation of intracellular cAMP, which is a key second messenger of signal transduction.<sup>21</sup> It triggers the transcription of downstream genes, including *HGF*, under the PKA signaling pathway.<sup>10</sup> Indeed, the phosphorylation of CREB could be detected in the cells treated with cAMP inducer like forskolin (Figure 3B), which is known to activate the adenylyl cyclase.<sup>22</sup> Our result showed that the phosphorylation of CREB was enhanced 15 min after the treatment of C3G and reduced to the basal level (Figure 3B). This rapid response was also observed in the previous

investigation.<sup>23</sup> Taken together, these results indicated that the activation of PKA pathway was involved in the mechanism of C3G on HGF induction.

**C3G Enhanced Promoter Activity of CRE and cAMP Levels through Activation of  $\beta_2$ AR.** To further study on the effect of C3G in the PKA pathway, we examined whether C3G enhances the promoter activity of cAMP-response element (CRE), which is a target sequence of phosphorylated CREB.<sup>24</sup> Previously, we transfected NHDFs with the reporter plasmid DNA encoding the luciferase gene under the CRE element; however, the luciferase activity was not detected due to low transfection efficiency of NHDFs (data not shown). Thus, HEK293 cells were used for the investigation on the promoter activity. Initially, we measured the levels of CRE promoter activity in the presence of forskolin, C3G, and the combination of the two compounds by using HEK293 cells transiently expressing the reporter plasmid. As shown in Figure 4, C3G

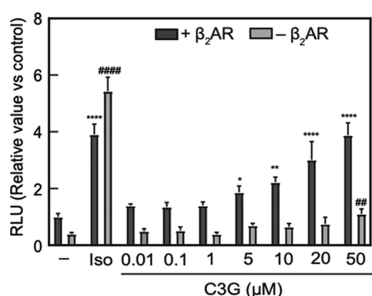


**Figure 4.** C3G enhanced promoter activity of CRE through the  $\beta_2$ AR signaling pathway. HEK293 cells were transiently co-transfected with pGL4.29 and pcDNA3.1- $\beta_2$ AR then seeded into a 96-well plate. Transfected cells were treated with vehicle (0.1% DMSO, shown as -), isoproterenol (10  $\mu$ M, shown as Iso), or C3G at the indicated concentrations for 24 h treatment. Luminescence value corresponding to CRE promoter activity was measured using cell lysates. Statistical analysis was conducted using one-way ANOVA (Tukey's test). Significant differences (\*\*\*\* $p$  < 0.0001, \*\* $p$  < 0.01, \* $p$  < 0.05) versus vehicle treatment group at cells co-transfected with pGL4.29 and pcDNA3.1- $\beta_2$ AR. Significant differences (##### $p$  < 0.0001, ### $p$  < 0.01) versus vehicle treatment group at cells transfected with pGL4.29.  $n$  = 5.

slightly increased the CRE promoter activity in HEK293 cells transfected with the reporter plasmid. In contrast to a single treatment of C3G, the CRE activity was synergistically increased in combination with C3G and forskolin (Figure S2), suggesting that the two compounds target different molecules for the activation of CRE. It motivated us to investigate the target of C3G by focusing on the different molecules other than adenylyl cyclase. We found that C3G dramatically enhanced the CRE activity in the presence of exogenous  $\beta_2$ -adrenergic receptor ( $\beta_2$ AR) (Figure 4), a representative member of G-protein-coupled receptor (GPCR). The increase of CRE activity by C3G was observed in a dose-dependent manner, suggesting that C3G functions as a  $\beta_2$ AR activator.

To further investigate the function of C3G on the  $\beta_2$ AR activation, we measured intracellular cAMP levels in  $\beta_2$ AR-expressing cells by using GloSensor technology that can detect the amount of cellular cAMP production with high sensitivity.<sup>25</sup> The binding of agonist to  $\beta_2$ AR subsequently activates adenylyl cyclase to induce cAMP production in cytosol.<sup>26</sup> Indeed, we observed the elevation of intracellular cAMP levels in the cells with or without exogenous expression of  $\beta_2$ AR when exposed to isoproterenol, which is known as nonselective agonist for  $\beta$  adrenergic receptor (Figure 5A,B). In contrast, C3G increased the cAMP levels in the cells only when  $\beta_2$ AR was exogenously expressed. This elevation of cAMP peaked at around 330 s after the treatment and returned to the basal level (Figure 5A), reflecting the fate of cAMP produced in the cells.<sup>27</sup> C3G also showed dose-response effect on the cAMP elevation in the presence of  $\beta_2$ AR (Figure 5B). Altogether, these results indicated that  $\beta_2$ AR was a potential target of C3G for the PKA activation.

**Comparison Study with Aglycon.** To gain insight into the interaction of C3G with  $\beta_2$ AR, we compared the biological effects of C3G with cyanidin, its aglycon derivative. Unlike C3G, cyanidin did not show the activation of CRE activity in HEK293 cells expressing  $\beta_2$ AR (Figure 6B). The same tendency was observed in the HGF production in NHDF cells (Figure 6A). These observations suggested that the glucoside moiety of C3G was important for the activation of  $\beta_2$ AR and HGF production.

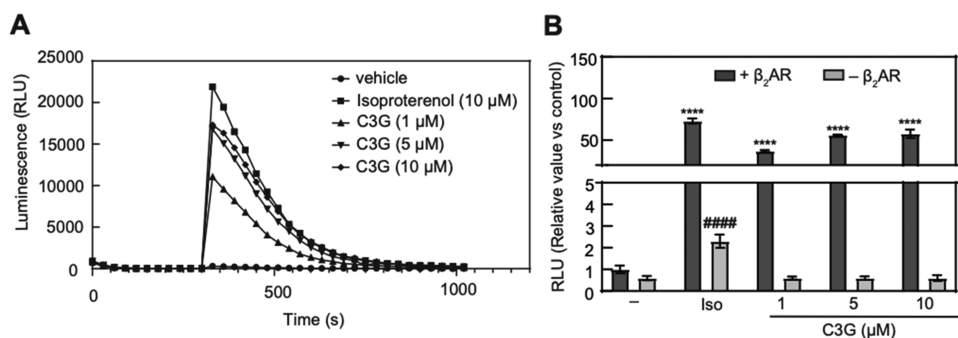


**Figure 5.** C3G increased intracellular cAMP levels through the  $\beta_2$ AR signaling pathway. (A) HEK293 cells were transiently co-transfected with pGloSensor-22F cAMP and pcDNA3.1- $\beta_2$ AR and then seeded into a 96-well plate. Transfected cells were treated with vehicle (0.1% DMSO), isoproterenol, or C3G at the indicated concentrations; then kinetic measurement of intracellular cAMP was performed. (B) Peak values of RLU based on kinetic assay in the transfected-HEK293 cells were shown. Statistical analysis was conducted using one-way ANOVA (Tukey's test). Significant difference (\*\*\*\* $p$  < 0.0001) versus vehicle treatment group on the cells co-transfected with pGloSensor-22F cAMP and pcDNA3.1- $\beta_2$ AR. Significant difference (##### $p$  < 0.0001) versus vehicle treatment group on the cells transfected with pGloSensor-22F cAMP.  $n$  = 3. Iso: isoproterenol (10  $\mu$ M).



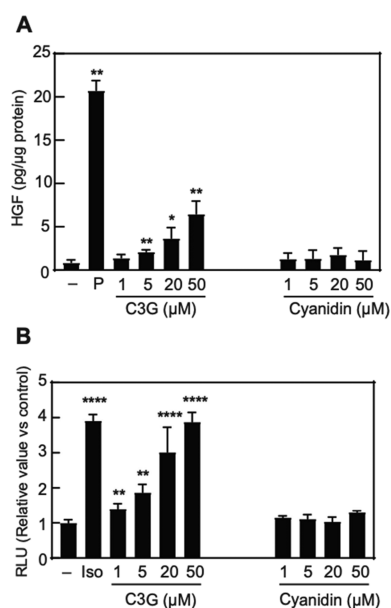


**Figure 6.** Comparison study with aglycon. (A) NHDF cells were treated with vehicle (0.1% DMSO, shown as -), PDGF-BB (25 ng/mL, shown as P), C3G, or cyanidin at the indicated concentrations for 120 h. The amount of HGF secreted into the culture medium was measured by ELISA assay. Statistical analysis was conducted using Student's t-test. Significance difference (\*\* $p < 0.01$ , \* $p < 0.05$ ) versus vehicle treatment group.  $n = 5$ . (B) HEK293 cells were transiently co-transfected with pGL4.29 and pcDNA3.1- $\beta_2$ AR and then seeded into a 96-well plate. Transfected cells were treated with vehicle (0.1% DMSO, shown as -), isoproterenol (10  $\mu$ M, shown as Iso), C3G, or cyanidin at the indicated concentrations for 24 h treatment. Luminescence was measured using cell lysates. Statistical analysis was conducted using one-way ANOVA (Tukey's test). Significant difference (\*\*\*\* $p < 0.0001$ , \*\* $p < 0.01$ ) versus vehicle treatment group.  $n = 5$ .

## DISCUSSION

Recent investigations highlighted the therapeutic potential of HGF on various diseases including neurodegenerative and skin-related diseases, as well as cancers.<sup>28–30</sup> Several preclinical studies demonstrated that the administration of recombinant HGF or injection of HGF expression vector to the patient was discovered as promising approaches for the attenuation of disease process.<sup>8,31,32</sup> Thus, a pharmacological approach using small molecules that function as a HGF inducer is also thought to be useful for disease prevention or treatment. Here, we found that C3G, an anthocyanidin derivative, stimulated HGF production in NHDF cells by upregulation of transcription of *HGF* gene without cytotoxicity at several concentrations. So far, many researchers focused on the flavonoids including anthocyanidins to modulate the downstream signaling of growth factors including HGF;<sup>33–35</sup> however, there are few reports on the enhancement of growth factor production by using flavonoids including anthocyanidin.

Previously, Ono et al. demonstrated that the extract of bitter melon pulp enhanced HGF production through the activation of MAPK pathway.<sup>12</sup> While they suggested that active substances may be nonproteinous macromolecules with the mass of around 14,000 Da, it has not been identified yet. We previously reported that daphnane diterpenes, known as PKC modulators, enhanced the HGF production in NHDF cells.<sup>14</sup> In addition, some phenylethanoids and phenylpropanoids, which bear the catechol moiety in their structure, also act as

HGF inducers;<sup>13</sup> however, the detailed mechanism of these compounds has not been clarified. In the present study, we demonstrated that C3G mainly regulated PKA pathway to upregulate the transcription of *HGF* gene under the CRE promoter. Our result is supported by previous transcriptome analysis that demonstrated upregulation of the downstream genes of PKA pathway by the treatment of C3G in human amniotic epithelial cells.<sup>36</sup>

Another important finding of this study is that C3G functions as a  $\beta_2$ AR activator for the regulation of the PKA pathway.  $\beta_2$ AR is a member of G protein-coupled receptor, which is involved in the regulation of relaxation of airway smooth muscle and glucose uptake in several insulin-sensitive tissues.<sup>37,38</sup> But the relationship between  $\beta_2$ AR activation and HGF production has rarely been investigated. Here, we showed that C3G stimulated the intracellular cAMP production and CRE promoter activity specifically in the presence of  $\beta_2$ AR (Figures 4 and 5), suggesting that C3G directly targeted  $\beta_2$ AR. It may also complement the previous findings of biological effects of C3G, which correlate with cAMP elevation through upregulation of PGC1- $\alpha$  and induction of preadipocyte differentiation.<sup>39,40</sup>

The modes of  $\beta_2$ AR activation are different among the functions of ligands. Binding of a full agonist such as isoproterenol to  $\beta_2$ AR causes the activation and dissociation of G proteins, leading to the stimulation of second messenger molecules production including the synthesis of cAMP by adenylyl cyclase.<sup>41</sup> Other type of ligands such as carvedilol does not cause the activation of G protein and preferentially regulate  $\beta$ -arrestin signaling.<sup>42</sup> Given that C3G stimulated cAMP levels and CRE promoter activity in a  $\beta_2$ AR-dependent manner, we assumed that C3G functions as an agonist of  $\beta_2$ AR. The compounds that bear the catechol group such as isoproterenol exhibit full agonism of  $\beta_2$ AR.<sup>43,44</sup> These catechol groups serve as hydrogen bond donors to Ser203<sup>5,42</sup> and Ser207<sup>5,46</sup> in the  $\beta_2$ AR to cause the arrangement of TM5 and TM 3/6. While we assume that the catechol group of C3G is likely to exhibit similar interaction, other substructures may play distinct roles compared with existing ligands. The major class of  $\beta_2$ AR agonists, including epinephrine, isoproterenol, and formoterol, possess secondary alcohol and amine groups conjugated with catechol, which interacts with Asp113<sup>3,32</sup> and Asn312<sup>7,39</sup>, whereas C3G does not have these functional groups in the structure. Instead, 3-glucoside moiety may play an important role for the agonistic activity and possibly interaction with  $\beta_2$ AR, as shown in comparison study with aglycon (Figure 6A,B). Previously, Kato et al. reported that higenamine 4'-*O*- $\beta$ -D-glucoside, a plant-derived tetraisoquinoline compound, enhanced glucose uptake in L6 cells.<sup>45</sup> They also discussed the potential function of the glucoside compound as a  $\beta_2$ AR binder. Although biophysical investigations such as crystal structural analysis or binding assay and further structure–activity relationship study are needed, these suggest the potential role of glucoside moiety for the interaction with  $\beta_2$ AR.

In conclusion, this study discovered the stimulation effect of C3G on HGF productions in NHDF cells through the activation of PKA pathway possibly by targeting the  $\beta_2$ AR. While we showed the potential importance of glucoside moiety of C3G for binding to  $\beta_2$ AR, other chemical modifications of anthocyanidin are also of interest from the perspective of dietary intake<sup>46</sup> as well as the ligand–receptor interaction. Further studies on the pharmacological properties are

warranted to assess the therapeutic potential of C3G and its chemical derivatives on tissue regeneration and wound healing.

## METHODS

**Test Compounds.** Test compounds used in this study were purchased from the following manufacturers: cyanidin 3-glucoside (Fuji Film Wako Pure Chemical Corporation, Japan, #633-42451NS380101), cyanidin chloride (Fuji Film Wako Pure Chemical Corporation, Japan, #030-21961), platelet-derived growth factor-BB (PDGF-BB) (Fuji Film Wako Pure Chemical Corporation, Japan, #166-19743), forskolin (Nacalai Tesque, Inc., Japan, #16384-84), isoproterenol (Nacalai Tesque, Inc., Japan, #19703-04), and H89 (Cayman Chemical, United States, #10010556).

**Cell Culture.** NHDF cells, purchased from Kurabo Co., Ltd. (Japan), were cultured in Dulbecco's modified Eagle's medium (DMEM) (Sigma-Aldrich, Co. LLC., United States, #D5796) containing 10% fetal bovine serum (Gibco, Thermo Fisher Scientific, United States) at 37 °C in humidified 5% CO<sub>2</sub> atmosphere. Human Embryonic Kidney 293 cells (HEK293), provided from RIKEN Bioresource Research Center (Japan), were cultured in DMEM containing 10% fetal bovine serum and 1% of 100 U/mL Penicillin and 100 μg/mL streptomycin (Sigma-Aldrich, Co., LLC., United States, #11074440001) at 37 °C in humidified 5% CO<sub>2</sub> atmosphere.

**Cell Viability Assay.** Confluent NHDF cells were seeded into 96-well plate at a density of  $1 \times 10^4$  cells/well. The cells were treated with C3G for 24, 48, or 120 h. After treatment, the old medium was replaced with the fresh medium. Subsequently, 3-(4,5-dimethylthiazol-2-yl)-2,5-diphenyltetrazolium bromide (MTT; Dojindo, Japan, #M009) solution (5 mg/mL) was added to the cell culture. After formazan crystals were observed, 100 μL of 10% SDS was added to each well, followed by incubation overnight. Then, the absorbance was measured at 570 nm using a microplate reader (Varioskan Lux, Thermo Fisher Scientific, United States).

**Determination of HGF Levels in Conditioned Media.** NHDF cells were seeded in a 96-well plate (Nunc, Denmark) at a density of  $1 \times 10^4$  cells/well and incubated overnight. The cells were treated with test samples dissolved in 100 μL of DMEM supplemented with 0.5% FBS. After treatment, the conditioned medium was collected for the quantification of HGF. Cell layers were washed with phosphate-buffered saline (PBS) and lysed with 0.5% Triton X-100 in PBS. Then, the amount of cellular protein was quantified using a BCA assay (Takara Bio, Inc., Japan #T9300A).

The sandwich human HGF ELISA was performed at room temperature. Briefly, 96-well plates were coated with anti-human HGF monoclonal antibody (0.2 μg/mL, diluted in PBS) (R&D Systems, Inc., United States, #294-HG-100/CF) and incubated overnight at 4 °C. The wells were washed with 0.05% Tween 20 in PBS and incubated with PBS containing 1% BSA, 5% Tween 20, and 5% sucrose for 1 h. After washing, the conditioned medium was added to the wells. At the same time, human HGF (R&D Systems, Inc., United States, #294-HG-005) for the standard curve was also added within the range of 0–50 ng/mL. After 2 h incubation, the wells were washed and incubated with biotinylated goat antihuman HGF antibody (250 ng/mL, diluted in PBS) (R&D Systems, Inc., United States, #BAF294) for 90 min incubation. After washing, streptavidine HRP conjugate (200 ng/mL, diluted in PBS) (Sigma-Aldrich, Co., LLC., United States, #RABHRP3) was added and incubated for 30 min. The wells were washed, and

the substrate solution containing ABTS (2,2'-azino-di-(3-ethylbenzthiazoline sulfonic acid), 0.3 mg/mL) (Sigma-Aldrich, #10102946001) mixed with H<sub>2</sub>O<sub>2</sub> at ratio 1:1000 was added and then incubated for another 30 min. Stop solution (1 M H<sub>2</sub>SO<sub>4</sub>) was added, and the optical density of each well was determined at 450 nm using a microplate reader (Varioskan Lux, Thermo Fisher Scientific, United States). The HGF levels were expressed as pg/μg cellular protein.

**Measurement of mRNA Abundance of HGF Gene.** NHDF cells were treated with test samples for 48 h, and total RNA was collected by using the ISOGEN kit (Nippon Gene Co., Ltd., Japan, #311-02501). Reverse transcription of RNA was performed using Superscript VILO Master Mix (Thermo Fisher Scientific, United States, #11755050). Real-time PCR analysis was conducted by using THUNDERBIRD SYBR qPCR Mix (Toyobo, Co., Ltd., Japan, #QPS-201 T) and analyzed on 7500 FAST Real-Time PCR (Applied Biosystems, United States). Gene expression data were normalized to that for β-actin. Primer sequences were as follows: HGF, forward: 5'-ACGAACACAGCTTTTTGCCTT-3', HGF, reverse 5'-AACTCTCCCCATTGCAGGTC-3', β-actin, forward 5'-CTGTGGCATCCACGAACTACC-3', β-actin, reverse 5'-GCAGTGATCTCCTTCTGCATCC-3'.

**Determination of Phosphorylated CREB.** NHDF cells were treated with test samples and then lysed in RIPA buffer (Nacalai Tesque, Inc., Japan, #16488-34) mixed with 1% phosphatase inhibitor cocktail (Nacalai Tesque, Inc., Japan, #07575-51). Total cellular protein samples were boiled in 5 × SDS sample buffer for 5 min, separated by 10% SDS-PAGE, and transferred to Immobilon-P PVDF membrane (Merck Millipore, United States, #IPFL00010). The blot was incubated with a blocking solution (2% BSA in TBS/T solution) and then probed with anti-pCREB (1:1000, Cell Signaling Technology, United States, #9198S) or anti-GAPDH (1:3000, Thermo Fisher Scientific, United States, #MA5-15738). Horseradish peroxidase (HRP)-conjugated anti-rabbit (Cell Signaling Technology, United States, #7074) or anti-mouse secondary antibodies (Cell Signaling Technology, United States, #7076) were used at a 1:3000 dilution. Immunoreactive bands were visualized using immobilon western chemiluminescent HRP substrate (Merck Millipore, United States, #WBKLS0500) using LuminoGraphI (WSE-6100, ATTO Corporation, Japan).

**Construction of pcDNA3.1-β<sub>2</sub>AR.** DNA fragment encoding β<sub>2</sub>AR was amplified from the plasmid (Addgene, #14697) and cloned into a pcDNA3.1 vector (Invitrogen, United States) by using the seamless ligation cloning extract (SLiCE) method.<sup>47</sup>

**CRE Reporter Assay.** HEK293 cells were transfected with pGL4.29 (Promega Corporation, United States) and pcDNA3.1-β<sub>2</sub>AR using Hilymax (Dojindo, Japan, #H357). Transfected cells were treated with test samples for 24 h. CRE promoter activity was measured using a luciferase assay system (Promega Corporation, United States, #E1500). Luminescence values (RLU) corresponding to CRE promoter activity were quantified using a microplate reader (Varioskan Lux, Thermo Fisher Scientific, United States).

**Measurement of Intracellular cAMP Levels.** HEK293 cells were transfected with pGloSensor-22F cAMP (Promega Corporation, United States) and pcDNA3.1-β<sub>2</sub>AR using Hilymax. Intracellular cAMP levels were measured by using GloSensor cAMP assay (Promega Corporation, United States, #E1290) according to the manufacturer's protocol. Briefly,

transfected cells were equilibrated with CO<sub>2</sub> independent medium (Thermo Fisher Scientific, United States, #18045088) containing 10% FBS and 2% GloSensor cAMP reagent. After incubating for 2 h in room temperature, the cells were exposed to the test samples and subjected to kinetic measurement of luminescence for the determination of cAMP levels by a microplate reader (Varioskan Lux, Thermo Fisher Scientific, United States).

**Statistical Analysis.** Statistical analyses were performed using GraphPad Prism9. Methods and representative symbols are described in the legends of the figures. Symbols mean significant differences from mean values of indicated numbers of independent experiments. A paired Student's *t*-test or one-way ANOVA was used to compare different variables between two or more experimental groups, respectively. For all analyses, *p*-values below 0.05 were considered statistically significant and were indicated in the legends of the figures.

## ■ ASSOCIATED CONTENT

### SI Supporting Information

The Supporting Information is available free of charge at <https://pubs.acs.org/doi/10.1021/acsomega.2c02659>.

Effect of C3G on the viability of NHDF cells; effect of C3G on promoter activity of CRE (PDF)

## ■ AUTHOR INFORMATION

### Corresponding Author

Yusaku Miyamae – Faculty of Life and Environmental Sciences, Tsukuba, Ibaraki 305-8572, Japan; [orcid.org/0000-0002-8102-4391](https://orcid.org/0000-0002-8102-4391); Phone: +81-29-853-6043; Email: [myamae.yusaku.fw@u.tsukuba.ac.jp](mailto:myamae.yusaku.fw@u.tsukuba.ac.jp)

### Authors

Annis Krama – Life Science Innovation, School of Integrative and Global Majors, Tsukuba, Ibaraki 305-8572, Japan

Natsu Tokura – Agro-Bioresources Science and Technology, Life and Earth Sciences, Tsukuba, Ibaraki 305-8572, Japan

Hiroko Isoda – Faculty of Life and Environmental Sciences, Tsukuba, Ibaraki 305-8572, Japan; Alliance for Research on the Mediterranean and North Africa, Tsukuba, Ibaraki 305-8572, Japan

Hideyuki Shigemori – Faculty of Life and Environmental Sciences, Tsukuba, Ibaraki 305-8572, Japan; Microbiology Research Center for Sustainability, University of Tsukuba, Tsukuba, Ibaraki 305-8572, Japan

Complete contact information is available at: <https://pubs.acs.org/doi/10.1021/acsomega.2c02659>

### Notes

The authors declare no competing financial interest.

## ■ ACKNOWLEDGMENTS

We thank Dr. Daisuke Matsuura (Bathclin Corporation) for the helpful discussion about culture of NHDF cells.

## ■ REFERENCES

- (1) Nakamura, T.; Teramoto, H.; Ichihara, A. Purification and characterization of a growth factor from rat platelets for mature parenchymal hepatocytes in primary cultures. *Proc. Natl. Acad. Sci. U. S. A.* **1986**, *83*, 6489–6493.
- (2) Mizuno, K.; Takehara, T.; Nakamura, T. Proteolytic activation of a single-chain precursor of hepatocyte growth factor by extracellular serine-protease. *Biochem. Biophys. Res. Commun.* **1992**, *189*, 1631–1638.
- (3) Bussolino, F.; Di Renzo, M. F.; Ziche, M.; Bocchietto, E.; Olivero, M.; Naldini, L.; Gaudino, G.; Tamagnone, L.; Coffer, A.; Comoglio, P. M. Hepatocyte growth factor is a potent angiogenic factor which stimulates endothelial cell motility and growth. *J. Cell Biol.* **1992**, *119*, 629–641.
- (4) Kato, T. Biological roles of hepatocyte growth factor-Met signaling from genetically modified animals. *Biomed. Rep.* **2017**, *7*, 495–503.
- (5) Matsumoto, K.; Funakoshi, H.; Takahashi, H.; Sakai, K. HGF-Met Pathway in Regeneration and Drug Discovery. *Biomedicines* **2014**, *2*, 275–300.
- (6) Dunsmore, S. E.; Rubin, J. S.; Kovacs, S. O.; Chedid, M.; Parks, W. C.; Welgus, H. G. Mechanisms of hepatocyte growth factor stimulation of keratinocyte metalloproteinase production. *J. Biol. Chem.* **1996**, *271*, 24576–24582.
- (7) Miura, Y.; Van Bich, N. T.; Furuya, M.; Hasegawa, H.; Takahashi, S.; Katagiri, N.; Hongu, T.; Funakoshi, Y.; Ohbayashi, N.; Kanaho, Y. The small G protein Arf6 expressed in keratinocytes by HGF stimulation is a regulator for skin wound healing. *Sci. Rep.* **2017**, *7*, 46649.
- (8) Ishigaki, A.; Aoki, M.; Nagai, M.; Warita, H.; Kato, S.; Kato, M.; Nakamura, T.; Funakoshi, H.; Itoyama, Y. Intrathecal delivery of hepatocyte growth factor from amyotrophic lateral sclerosis onset suppresses disease progression in rat amyotrophic lateral sclerosis model. *J. Neuropathol. Exp. Neurol.* **2007**, *66*, 1037–1044.
- (9) Zhao, L. J.; Wang, Z. T.; Ma, Y. H.; Zhang, W.; Dong, Q.; Yu, J. T.; Tan, L. Alzheimer's Disease Neuroimaging Initiative. Associations of the cerebrospinal fluid hepatocyte growth factor with Alzheimer's disease pathology and cognitive function. *BMC Neurol.* **2021**, *21*, 387.
- (10) Matsunaga, T.; Gohda, E.; Takebe, T.; Wu, Y. L.; Iwao, M.; Kataoka, H.; Yamamoto, I. Expression of hepatocyte growth factor is up-regulated through activation of a cAMP-mediated pathway. *Exp. Cell Res.* **1994**, *210*, 326–335.
- (11) Chattopadhyay, N.; Tfelt-Hansen, J.; Brown, E. M. PKC, p42/44 MAPK and p38 MAPK regulate hepatocyte growth factor secretion from human astrocytoma cells. *Brain Res. Mol. Brain Res.* **2002**, *102*, 73–82.
- (12) Ono, T.; Tsuji, T.; Sakai, M.; Yukizaki, C.; Ino, H.; Akagi, I.; Hiramatsu, K.; Matsumoto, Y.; Sugiura, Y.; Uto, H.; Tsubouchi, H.; Gohda, E. Induction of hepatocyte growth factor production in human dermal fibroblasts and their proliferation by the extract of bitter melon pulp. *Cytokine+* **2009**, *46*, 119–126.
- (13) Kurisu, M.; Nakasone, R.; Miyamae, Y.; Matsuura, D.; Kanatani, H.; Yano, S.; Shigemori, H. Induction of hepatocyte growth factor production in human dermal fibroblasts by caffeic acid derivatives. *Biol. Pharm. Bull.* **2013**, *36*, 2018–2021.
- (14) Nakasone, R.; Kurisu, M.; Onodera, M.; Miyamae, Y.; Matsuura, D.; Kanatani, H.; Yano, S.; Shigemori, H. Promoting Effects on Hepatocyte Growth Factor Production of Daphnane Diterpenoids from *Daphne odora*. *Heterocycles* **2013**, *87*, 1087.
- (15) White, B. L.; Howard, L. R.; Prior, R. L. Proximate and polyphenolic characterization of cranberry pomace. *J. Agric. Food Chem.* **2010**, *58*, 4030–4036.
- (16) Sukprasansap, M.; Chanvorachote, P.; Tencomnao, T. Cyanidin-3-glucoside activates Nrf2-antioxidant response element and protects against glutamate-induced oxidative and endoplasmic reticulum stress in HT22 hippocampal neuronal cells. *BMC Complementary Med. Ther.* **2020**, *20*, 46.
- (17) Serra, D.; Paixão, J.; Nunes, C.; Dinis, T. C.; Almeida, L. M. Cyanidin-3-glucoside suppresses cytokine-induced inflammatory response in human intestinal cells: comparison with 5-aminosalicylic acid. *PLoS One* **2013**, *8*, No. e73001.
- (18) Tsuda, T.; Horio, F.; Uchida, K.; Aoki, H.; Osawa, T. Dietary cyanidin 3-O-beta-D-glucoside-rich purple corn color prevents obesity and ameliorates hyperglycemia in mice. *J. Nutr.* **2003**, *133*, 2125–2130.



- (19) Gohda, E.; Matsunaga, T.; Kataoka, H.; Takebe, T.; Yamamoto, I. Induction of hepatocyte growth factor in human skin fibroblasts by epidermal growth factor, platelet-derived growth factor and fibroblast growth factor. *Cytokine* **1994**, *6*, 633–640.
- (20) Chijiwa, T.; Mishima, A.; Hagiwara, M.; Sano, M.; Hayashi, K.; Inoue, T.; Naito, K.; Toshioka, T.; Hidaka, H. Inhibition of forskolin-induced neurite outgrowth and protein phosphorylation by a newly synthesized selective inhibitor of cyclic AMP-dependent protein kinase, N-[2-(p-bromocinnamylamino)ethyl]-5-isoquinolinesulfonamide (H-89), of PC12D pheochromocytoma cells. *J. Biol. Chem.* **1990**, *265*, 5267–5272.
- (21) Shaywitz, A. J.; Greenberg, M. E. CREB: a stimulus-induced transcription factor activated by a diverse array of extracellular signals. *Annu. Rev. Biochem.* **1999**, *68*, 821–861.
- (22) Curtin, B. F.; Pal, N.; Gordon, R. K.; Nambiar, M. P. Forskolin, an inducer of cAMP, up-regulates acetylcholinesterase expression and protects against organophosphate exposure in neuro 2A cells. *Mol. Cell. Biochem.* **2006**, *290*, 23–32.
- (23) Mayr, B. M.; Canettieri, G.; Montminy, M. R. Distinct effects of cAMP and mitogenic signals on CREB-binding protein recruitment impart specificity to target gene activation via CREB. *Proc. Natl. Acad. Sci. U. S. A.* **2001**, *98*, 10936–10941.
- (24) Cha-Molstad, H.; Keller, D. M.; Yochum, G. S.; Impey, S.; Goodman, R. H. Cell-type-specific binding of the transcription factor CREB to the cAMP-response element. *Proc. Natl. Acad. Sci. U. S. A.* **2004**, *101*, 13572–13577.
- (25) Fan, F.; Binkowski, B. F.; Butler, B. L.; Stecha, P. F.; Lewis, M. K.; Wood, K. V. Novel genetically encoded biosensors using firefly luciferase. *ACS Chem. Biol.* **2008**, *3*, 346–351.
- (26) Johnstone, T. B.; Agarwal, S. R.; Harvey, R. D.; Ostrom, R. S. cAMP Signaling Compartmentation: Adenylyl Cyclases as Anchors of Dynamic Signaling Complexes. *Mol. Pharmacol.* **2018**, *93*, 270–276.
- (27) Nikolaev, V. O.; Lohse, M. J. Monitoring of cAMP synthesis and degradation in living cells. *Physiology* **2006**, *21*, 86–92.
- (28) Kadoyama, K.; Funakoshi, H.; Ohya, W.; Nakamura, T. Hepatocyte growth factor (HGF) attenuates gliosis and motoneuronal degeneration in the brainstem motor nuclei of a transgenic mouse model of ALS. *Neurosci. Res.* **2007**, *59*, 446–456.
- (29) Baek, J. H.; Birchmeier, C.; Zenke, M.; Hieronymus, T. The HGF receptor/Met tyrosine kinase is a key regulator of dendritic cell migration in skin immunity. *J. Immunol.* **2012**, *189*, 1699–1707.
- (30) Owusu, B. Y.; Galemno, R.; Janetka, J.; Klampfer, L. Hepatocyte Growth Factor, a Key Tumor-Promoting Factor in the Tumor Microenvironment. *Cancers* **2017**, *9*, 35.
- (31) Nagoshi, N.; Tsuji, O.; Kitamura, K.; Suda, K.; Maeda, T.; Yato, Y.; Abe, T.; Hayata, D.; Matsumoto, M.; Okano, H.; Nakamura, M. Phase I/II Study of Intrathecal Administration of Recombinant Human Hepatocyte Growth Factor in Patients with Acute Spinal Cord Injury: A Double-Blind, Randomized Clinical Trial of Safety and Efficacy. *J. Neurotrauma* **2020**, *37*, 1752–1758.
- (32) Barć, P.; Antkiewicz, M.; Śliwa, B.; Baczyńska, D.; Witkiewicz, W.; Skóra, J. P. Treatment of Critical Limb Ischemia by pIRES/VEGF165/HGF Administration. *Ann. Vasc. Surg.* **2019**, *60*, 346–354.
- (33) Labbé, D.; Provençal, M.; Lamy, S.; Boivin, D.; Gingras, D.; Béliveau, R. The flavonols quercetin, kaempferol, and myricetin inhibit hepatocyte growth factor-induced medulloblastoma cell migration. *J. Nutr.* **2009**, *139*, 646–652.
- (34) Gao, F.; Deng, G.; Liu, W.; Zhou, K.; Li, M. Resveratrol suppresses human hepatocellular carcinoma via targeting HGF-c-Met signaling pathway. *Oncol. Rep.* **2017**, *37*, 1203–1211.
- (35) Syed, D. N.; Afaq, F.; Sarfaraz, S.; Khan, N.; Kedlaya, R.; Setaluri, V.; Mukhtar, H. Delphinidin inhibits cell proliferation and invasion via modulation of Met receptor phosphorylation. *Toxicol. Appl. Pharmacol.* **2008**, *231*, 52–60.
- (36) Takahashi, S.; Ferdousi, F.; Zheng, Y. W.; Oda, T.; Isoda, H. Human Amniotic Epithelial Cells as a Tool to Investigate the Effects of Cyanidin 3-O-Glucoside on Cell Differentiation. *Int. J. Mol. Sci.* **2021**, *22*, 3768.
- (37) Guo, M.; Pascual, R. M.; Wang, S.; Fontana, M. F.; Valancius, C. A.; Panettieri, R. A., Jr.; Tilley, S. L.; Penn, R. B. Cytokines regulate beta-2-adrenergic receptor responsiveness in airway smooth muscle via multiple PKA- and EP2 receptor-dependent mechanisms. *Biochemistry* **2005**, *44*, 13771–13782.
- (38) Nevzorova, J.; Evans, B. A.; Bengtsson, T.; Summers, R. J. Multiple signalling pathways involved in beta2-adrenoceptor-mediated glucose uptake in rat skeletal muscle cells. *Br. J. Pharmacol.* **2006**, *147*, 446–454.
- (39) Matsukawa, T.; Motojima, H.; Sato, Y.; Takahashi, S.; Villareal, M. O.; Isoda, H. Upregulation of skeletal muscle PGC-1 $\alpha$  through the elevation of cyclic AMP levels by Cyanidin-3-glucoside enhances exercise performance. *Sci. Rep.* **2017**, *7*, 44799.
- (40) Matsukawa, T.; Villareal, M. O.; Motojima, H.; Isoda, H. Increasing cAMP levels of preadipocytes by cyanidin-3-glucoside treatment induces the formation of beige phenotypes in 3T3-L1 adipocytes. *J. Nutr. Biochem.* **2017**, *40*, 77–85.
- (41) Penn, R. B.; Bond, R. A.; Walker, J. K. GPCRs and arrestins in airways: implications for asthma. *Handb. Exp. Pharmacol.* **2014**, *219*, 387–403.
- (42) Whalen, E. J.; Rajagopal, S.; Lefkowitz, R. J. Therapeutic potential of  $\beta$ -arrestin- and G protein-biased agonists. *Trends Mol. Med.* **2011**, *17*, 126–139.
- (43) Katritch, V.; Reynolds, K. A.; Cherezov, V.; Hanson, M. A.; Roth, C. B.; Yeager, M.; Abagyan, R. Analysis of full and partial agonists binding to beta2-adrenergic receptor suggests a role of transmembrane helix V in agonist-specific conformational changes. *J. Mol. Recognit.* **2009**, *22*, 307–318.
- (44) Wu, Y.; Zeng, L.; Zhao, S. Ligands of Adrenergic Receptors: A Structural Point of View. *Biomolecules* **2021**, *11*, 936.
- (45) Kato, E.; Kimura, S.; Kawabata, J. Ability of higenamine and related compounds to enhance glucose uptake in L6 cells. *Bioorg. Med. Chem.* **2017**, *25*, 6412–6416.
- (46) Araki, R.; Yada, A.; Ueda, H.; Tominaga, K.; Isoda, H. Differences in the Effects of Anthocyanin Supplementation on Glucose and Lipid Metabolism According to the Structure of the Main Anthocyanin: A Meta-Analysis of Randomized Controlled Trials. *Nutrients* **2021**, *13*, 2003.
- (47) Motohashi, K. A simple and efficient seamless DNA cloning method using SLiCE from Escherichia coli laboratory strains and its application to SLiP site-directed mutagenesis. *BMC Biotechnol.* **2015**, *15*, 47.